Journal of Brilliant Engineering 3 (2025) 41049
Brilliant Engineering
journal home: www.acapublishing.com/journals/4/ben

Research Article

Development of a Flexible, Shape-Adaptive and Waterproof Cementitious Composite Reinforced with 3D Textile

Kerem Aybar*[1], Serdal Ünal[2], Ömer Karagöz[3], Mehmet Canbaz[4]
[1]Eskişehir Osmangazi University, Metallurgical and Mat. Eng. Dep., Eskisehir, Turkey
[2,3,4]Eskişehir Osmangazi University, Civil Engineering Department, Eskisehir, Turkey

Keywords

3D textile reinforced composite,
Flexible cementitious material,
Shape-adaptive construction material,
Dynamic and static tensile behavior,
Bending strength.

Abstract

In this study, a flexible, shape-adaptive, and waterproof cementitious composite was developed by integrating 3D textile reinforcement with a specialized waterproofing membrane. This study aims to develop a next-generation building material that is lightweight, ductile, and resistant to bending and tensile forces, while also offering protection against water ingress. During the production process, carefully cut 3D textiles were placed into wooden molds and fully impregnated with CEM I type white cement, ensuring complete saturation of the textile structure. A waterproofing membrane was then applied as a protective surface layer to enhance durability and water resistance. After curing periods of 7 and 28 days under standard conditions, extensive mechanical testing was performed, including flexural strength, unit weight measurement, and both static and dynamic tensile tests on samples sized 30×30 cm and 10×30 cm. The experimental results demonstrated that despite its lightweight nature (approximately 0.87–0.88 kg/dm³), the composite achieved a high flexural strength of up to 16.95 MPa and tensile strength reaching 17.92 MPa. Stress-strain analyses revealed a significant energy absorption capacity, with elongation at break values approaching 30%, indicating excellent toughness. These combined mechanical and functional characteristics position the developed composite as an innovative and promising alternative for architectural applications that demand flexibility, shape adaptability, and resilience against harsh environmental conditions such as moisture and mechanical stresses.

1. Introduction

Textile-reinforced cementitious composites have gained increasing attention in recent years due to their potential for use in lightweight, form-adaptive, and durable structural systems [1]. These systems are particularly advantageous in applications such as precast façade panels, tunnel linings, architectural shells, and infrastructure repairs, where conventional reinforcement techniques may be inadequate due to weight or geometric limitations [2]. The integration of textile reinforcements into cementitious matrices allows for the production of thin-section elements with improved tensile and flexural performance, making them suitable for both structural and non-structural applications [3]. In 3D textile-reinforced cementitious composites (TRCC), flexibility and tensile strength of textiles complement the matrix's compressive capacity [4,5]. Compared to traditional reinforced concrete, textile-based composites can exhibit superior crack control, ductility, and durability [6]. Particularly, 3D textiles offer enhanced mechanical interlocking and matrix penetration, improving composite integrity and post-crack behavior [7]. Moreover, the flexibility of the textile allows the composite to be formed into complex geometries, which opens up new possibilities in architectural and civil engineering design [8,9].

However, most existing research on textile-reinforced cementitious composites has focused mainly on conventional mechanical parameters, while the influence of textile type, structural geometry, and loading conditions on the composite's performance remains underexplored. Additionally, tensile and flexural behavior in textile concretes is often evaluated using simplified testing approaches, with limited systematic data available on strain-dependent behavior under static and dynamic loads. In this study, a flexible, shape-adaptive, and mechanically resilient thin-section cementitious composite was developed using 3D textile reinforcement. The material's unit weight, flexural strength, static and dynamic tensile strength, and strain-dependent behavior were thoroughly investigated, highlighting the performance evolution over time. This study addresses a critical gap in the literature regarding the mechanical characterization of textile-reinforced cementitious systems. Furthermore, most recent studies have overlooked two important factors that are critical for practical applications in architectural and infrastructure systems: impermeability and shape adaptation. While existing TRCC systems are structurally efficient, they typically require additional protective layers or coatings to achieve water impermeability, and their ability to adapt to complex geometries remains limited without compromising durability performance. In this context, this study presents an innovative approach that directly integrates an asphalt-based waterproofing membrane with 3D textile reinforcement. This combination not only preserves the mechanical advantages of TRCCs but also inherently endows the material with waterproofing properties and the ability to adapt to various surface shapes without requiring additional processing. Thus, by addressing both functional and structural requirements in a single material system, it fills an important gap in the existing literature and offers a promising solution for applications where mechanical performance, water resistance, and geometric flexibility must be achieved simultaneously.

In this study, specimens were tested after 7 and 28 days of curing to reveal the time-dependent development of mechanical performance. Unit weight, flexural strength, static and dynamic tensile strength, as well as the corresponding strain behaviors under different loading conditions

*Corresponding Author: kaybar@ogu.edu.tr
Received 01 Aug 2025; Revised 08 Aug 2025; Accepted 08 Aug 2025
https://doi.org/10.36937/ben.2025.41049

were analyzed in detail. In this respect, the study provides a comprehensive contribution to the literature by examining not only the ultimate strength of textile-reinforced cementitious systems but also their deformation capacity, sensitivity to loading rate, and strength development over time.

2. Testing Process

2.1. Test specimens and properties

The unmodified Portland cement CEM I 42.5R with the properties specified in Table 1 was used as the binder. The selection of CEM I 42.5R cement was based on its high early strength development and good workability, even at low water-to-cement ratios. These properties offer advantages for thin-section, shape-adaptive composites that require rapid setting.

Table 1. Properties of cements

Chemical Content (%)		Physical Properties	
SiO_2	19,8	Density (g/cm^3)	3,07
Al_2O_3	4,50	Specific Surface (cm^2/g)	3593
Fe_2O_3	3,12	Initial Setting (min)	165
CaO	62,8	Final Setting (min)	228
MgO	1,90	Expansion (mm)	1
K_2O	0,59	Compressive strength, MPa	
Na_2O	0,34	7 days	36.5
SO_3	3,19	28 days	52,2

Eskişehir tap water, whose properties are given in Table 2, was used as the mixing water.

Table 2. Properties of mix water

Chemical Content (mg/l)						Physical Properties	
Al	0,05	Cu	0,017	Ni	5,07	Conductivity (µS/cm)	628
NO3	11,2	Fe	0,006	K	6,8	Hardness (Fd^0)	30,11
NH4	0,05	Mn	0,016	As	1,19	pH	7,35

The composite used in production is reinforced with 3D air-permeable textile with a thickness of 6 mm, as shown in Figure 1. The properties of the 3D air-permeable textile are given in Table 3. The chosen fabric type was selected for its high tensile strength, flexibility, and strong adhesion to the cement matrix, thereby optimizing both mechanical performance and shape retention.

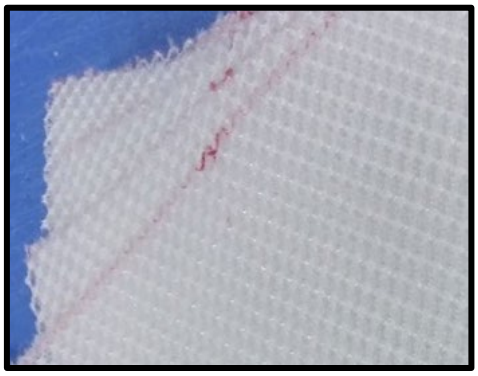

Figure 1. 3D Textile samples

Table 3. Properties of 3D spacer textiles [10, 11].

Components	Materials	Fineness (dtex)	Elongation (%)	Tensile strength (MPa)	Modulus of Elasticity (GPa)
Warp/Weft yarn_MF	Polyethylene terephthalate multifilaments	339	9.2	443	4.85
Warp/weft yarn_SF		396	6.1	731	11.39
Spacer yarn	Polyethylene terephthalate monofilaments	495	9.8	705	7.23
	Volume content of spacer yarn (%)	Volume fraction of warp-weft yarns (%)		Volume fraction of matrix (-)	
Warp	2.91	0.35		0.23	
Weft	2.91	0.35		0.23	

A 0.2 mm thick membrane reinforced with PVC on one side and fiber on the other, as shown in Figure 2, was used for waterproofing.

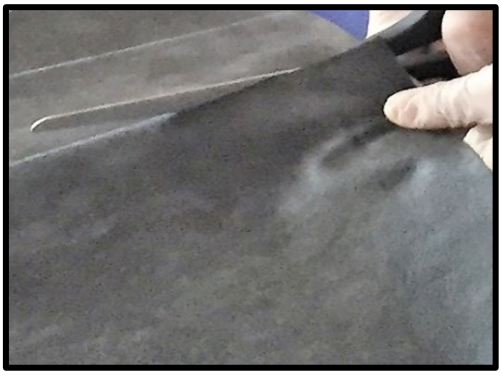

Figure 2. Appearance of waterproof material

2.2. Testing system and manufactured specimen

Pieces measuring 30 cm x 30 cm and 10 cm x 30 cm were cut from 3D textiles and waterproofing membranes. At least three samples were produced for each experiment and sample content. The cut pieces of 3D textile were placed inside a wooden mold. One side of the textile is tightly woven, allowing water to pass through but also retaining it; the other side has a porous structure. When placed in the mold, the tightly woven surface was brought to the bottom. This is because the aim is to allow cement to enter from the porous surface and prevent it from passing through to the bottom from the solid surface. CEM I type cement was spread on the textile surface, and a table vibrator was used to ensure the 3D textile was fully saturated. Excess cement on the upper surface was cleaned off. Then, adhesive was applied to the fibrous surface of the waterproofing membrane and it was attached to the sample surface. With membrane coating, cement is trapped between the membrane and the tight textile surface, resulting in textile concrete. The inverted samples were then soaked in water to saturate them. Textile concrete is watered from a tightly textile-covered surface to promote cement hydration and strength development. Since the surface is membrane-covered, the samples were turned upside down and water was sprayed onto the surface. These steps are illustrated in Figure 3.

Figure 3. Step-by-step manufacturing process of the 3D textile-reinforced cementitious composite, showing cutting of textile, placement in mold, cement application, and membrane attachment.

Specimens were weighed 7 and 28 days after production and underwent bending and tensile testing. As shown in Figure 4, the bending tests were conducted on 30 cm x 30 cm samples, and the tensile tests were conducted on 10 cm x 30 cm samples. In the bending test, deflections of up to 35 mm were observed. As shown in Figure 5, fracture occurred between the jaws in the tensile test. Both rapid and slow loading were performed in the tensile test. Rapid loading (crosshead speed 20 mm/min) is referred to as dynamic loading, while slow loading (crosshead speed 10 mm/min) is referred to as static loading.

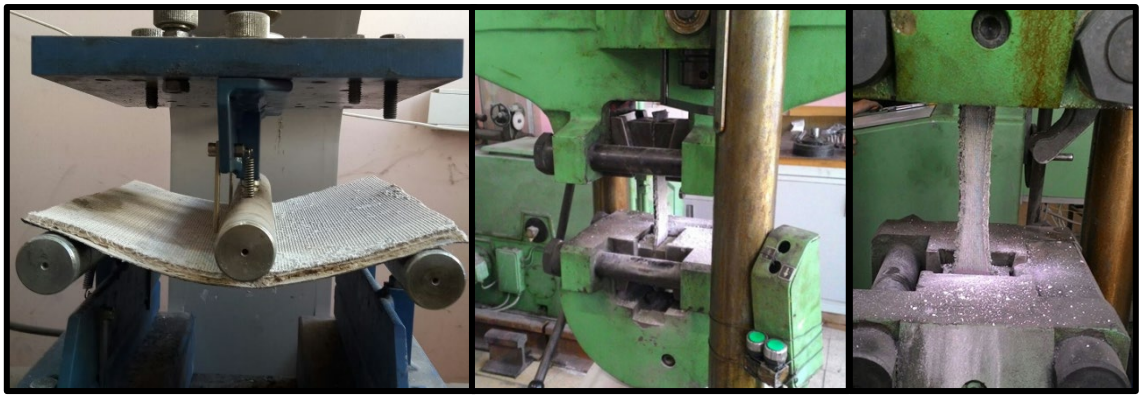

Figure 4. Conducting bending, tensile, and elongation tests on 3D textile-reinforced cement composite samples.

Figure 5. Appearance of 3D textile-reinforced cement composite samples after tensile testing.

3. Discussion

Figure 6 presents the unit weight and flexural strength results of the specimens at 7 and 28 days of curing. These two fundamental properties provide insights into both the density and mechanical performance of the composite material, playing a critical role in evaluating its functional and structural characteristics.

When examining the unit weight results, the value slightly decreased from 0.88 kg/dm³ at 7 days to 0.87 kg/dm³ at 28 days. This represents a minimal reduction of approximately 1.1%, which can be attributed to the evaporation of free water within the specimen. This minor loss aligns with the porous structure of the material. This small change means that water loss in the capillary voids of the textile concrete is limited and that it retains almost all of the water. Notably, the tightly woven bottom surface of the 3D textile, which restricts the upward migration of the cementitious matrix, may have caused an inhomogeneous hydration profile within the composite. Furthermore, the adhesion of the waterproof membrane to the top surface might have partially limited moisture escape, contributing to a slight loss in weight during the curing process. These findings also imply that the system maintains its volumetric stability, reducing the risk of drying shrinkage cracks.

In terms of flexural strength, a striking improvement was observed. The flexural strength increased from 1.68 MPa at 7 days to 16.95 MPa at 28 days, corresponding to an approximate rise of 908%. This dramatic increase indicates significant mechanical development of the composite throughout the hydration process. The low early-age strength can be explained by the insufficient bonding within the matrix and limited interaction between the cement paste and the textile fibers. However, as hydration progressed, the formation of calcium silicate hydrate (C-S-H) gels and enhanced mechanical interlocking with the porous surface of the 3D textile led to a substantial increase in strength. Additionally, the textile's ability to bridge cracks likely became more effective over time, enabling the material to sustain higher loads without failure as the fibers arrested crack propagation and maintained load transfer.

Overall, achieving high flexural strength with a low unit weight highlights the potential of this cementitious composite as a lightweight yet durable construction material. While low mechanical performance is a common issue in lightweight materials, the active role of the 3D textile in this system significantly mitigated this limitation. These results suggest that the developed composite is a promising candidate for use in lightweight structural elements that also require waterproofing functionality.

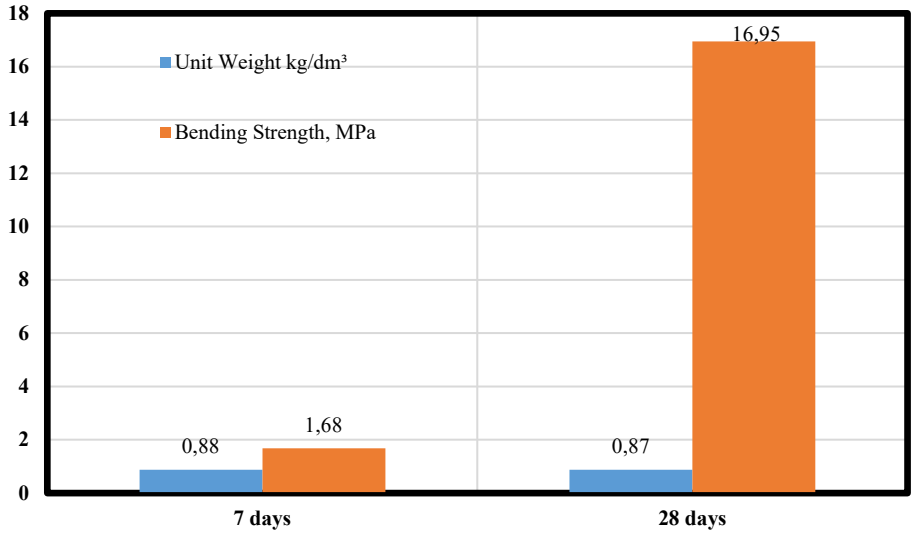

Figure 6. Unit weight and bending strength of 3D Textile composite specimens

Figure 7 shows the tensile strength results of the composites under both dynamic (fast loading) and static (slow loading) conditions at 7 and 28 days of curing. This test provides information on the stress rate sensitivity and time-dependent mechanical performance of textile-reinforced cement composites designed to operate under various loading conditions in practice.

At 7 days, the dynamic tensile strength was measured as 16.95 MPa, while the static tensile strength was slightly lower at 16.21 MPa. This marginal difference of approximately 4.5% suggests that even in the early stages of hydration, the material exhibits a moderate sensitivity to loading rate. The higher tensile strength under dynamic loading may be attributed to the viscoelastic behavior of the matrix and the fiber–matrix interface, which can respond more stiffly under rapid strain application. At early ages, the hydration products are still developing, and their microstructure may offer slightly more resistance to sudden loads due to limited time for crack initiation and propagation.

By 28 days, both dynamic and static tensile strengths increased slightly, reaching 17.92 MPa and 17.08 MPa respectively. The percentage increase from 7 to 28 days was approximately 5.7% for dynamic tensile strength and 5.4% for static tensile strength. This modest increase indicates that the majority of the tensile strength capacity had already been established by day 7, likely due to effective fiber bridging and early mechanical interlocking between the cementitious matrix and the 3D textile reinforcement. The limited gain in strength over time, compared to the dramatic flexural strength increase observed previously, suggests that the composite's tensile capacity is more reliant on the textile architecture and interfacial bonding than on matrix hydration alone.

The consistent superiority of dynamic tensile strength over static tensile strength at both ages demonstrates the composite's rate-dependent behavior. Under rapid loading, the energy dissipation mechanisms—such as microcrack deflection, fiber pull-out, and frictional sliding at the textile–matrix interface—are more active, resulting in higher apparent tensile strength. In contrast, under slow loading (static conditions), there is more time for microcracks to coalesce and propagate, which slightly reduces the peak tensile load the specimen can carry before failure.

In summary, the close values of dynamic and static tensile strength at both ages reflect a well-balanced and robust tensile behavior of the composite under different loading rates. This performance is particularly valuable for structural applications subject to both static and dynamic actions, such as façade panels, modular wall systems, or elements exposed to wind or impact forces. The 3D textile's role in ensuring continuity and energy absorption under varying strain rates further reinforces its suitability as a multifunctional reinforcement in flexible, durable, and shape-adaptive cementitious composites.

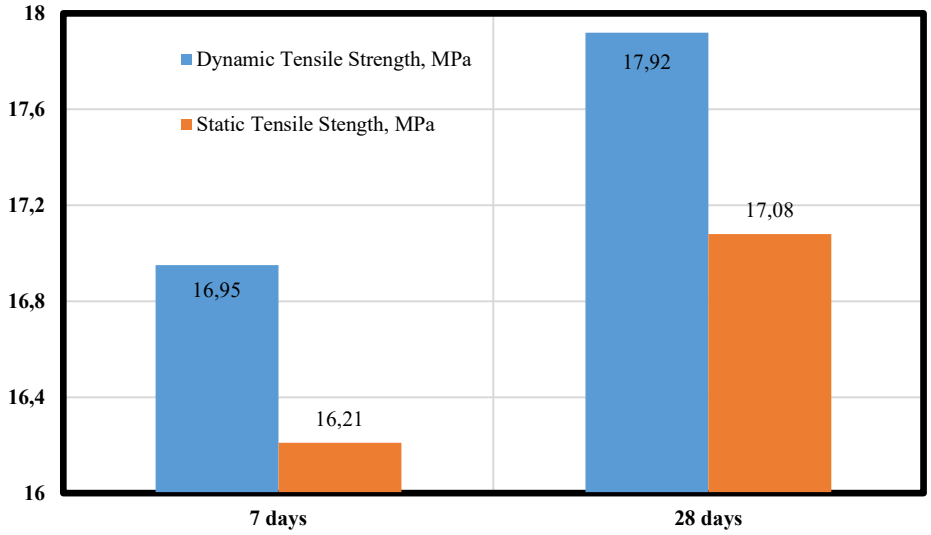

Figure 7. Tensile strength of 3D Textile composite specimens

Figure 8 presents the dynamic (fast loading) and static (slow loading) tensile elongation results of the specimens at 7 and 28 days of curing. In textile-reinforced cementitious systems, elongation performance depends not only on the matrix but also significantly on the textile architecture and fiber–matrix interfacial interactions.

At 7 days, the dynamic tensile elongation was recorded as 32.14%, while the static tensile elongation was slightly higher at 33.27%. These exceptionally high deformation capacities at an early age indicate that the composite can undergo significant strain prior to failure, exhibiting ductile behavior. This can be attributed to the relatively immature and less brittle cement matrix at this stage, allowing for greater flexibility, as well as the effective crack-bridging function of the 3D textile, which helps distribute the applied load along the fibers. Additionally, the presence of the waterproof membrane likely helped retain internal moisture, further delaying matrix embrittlement and supporting the observed ductility.

By day 28, a reduction in both dynamic and static elongation was observed. Dynamic elongation decreased to 21.43%, while static elongation dropped to 28.57%. This corresponds to a reduction of approximately 33% and 14%, respectively, compared to the 7-day values. While these elongation values are noticeable at an early age, it has been observed that rigidity increases with age due to the effects of hydration reactions, but the ability to change shape in response to sudden and slow reactions is maintained. These decreases indicate that as the matrix continues to cure and becomes denser and more brittle, the overall deformability of the composite diminishes. The more pronounced decrease in dynamic elongation suggests that under fast loading, the material becomes stiffer and less able to accommodate large deformations, potentially due to reduced time for microcrack development and fiber interaction.

The fact that static loading still allowed for higher elongation at 28 days demonstrates that slower crack propagation enables more extensive fiber deformation and energy dissipation. Mechanisms such as interfacial friction, fiber pull-out, and reorientation are more active under slow loading rates, contributing to the overall increase in elongation. This divergence between dynamic and static elongation values highlights the strain-rate sensitivity of the composite and its evolving ductility over time.

In conclusion, the high elongation values observed at both early and later ages confirm that the developed cementitious composite is not only strong but also highly deformable and energy-absorbing. These properties are particularly advantageous for applications requiring flexibility, impact resistance, or adaptive geometry, such as shell elements, kinetic surfaces, or damping structures. The synergy between the 3D textile and the moisture-retaining membrane provides both mechanical and environmental benefits, contributing positively to the composite's long-term performance.

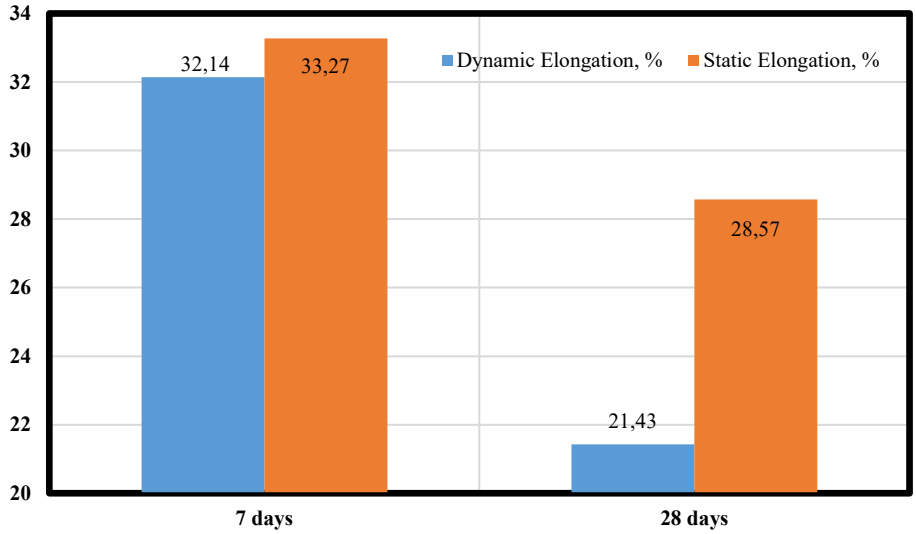

Figure 8. Elongation of 3D Textile composite specimens

Figure 9 presents the stress–strain curves of the specimens under static (slow loading) and dynamic (fast loading) conditions at 7 and 28 days of curing. Under 7-day static loading, the material quickly entered the elastic region, reaching approximately 14.27 MPa at 1.3% strain. Beyond this point, the curve exhibited nonlinear behavior, ultimately reaching a tensile strength of 16.21 MPa at 33.27% strain. This behavior indicates that the cement matrix had not fully rigidified yet, and the fiber–matrix interface maintained its flexibility, allowing the composite to sustain high deformation while carrying load.

Under 7-day dynamic loading, a similar elastic response was observed; however, at 1.2% strain, the stress was 14.77 MPa, increasing to 14.99 MPa at 7% strain. The ultimate strength of 16.95 MPa was achieved at 32.14% strain. These results suggest that under rapid loading, the fibers engage more actively, and the matrix has less time to crack, leading to a more immediate but higher strength response. However, compared to static loading, the deformation capacity is slightly reduced, indicating that ductility is limited under fast loading.

At 28 days under static loading, the material exhibited a stiffer behavior. At 0.5% strain, the stress was 7.04 MPa, rising to 15.11 MPa at 10% strain, and 16.12 MPa at 20% strain. The ultimate strength of 17.08 MPa was reached at 28.57% strain. Compared to early age, there is a significant increase in strength accompanied by a moderate reduction in deformation capacity. This suggests that the matrix becomes more brittle over time, but the textile reinforcement continues to control crack propagation and energy dissipation.

Under 28-day dynamic loading, a similar trend was observed, but with a notably lower deformation capacity. At 1% strain, the stress was 15.18 MPa, increasing to 15.96 MPa at 12% strain, and reaching a maximum strength of 17.92 MPa at 20% strain. These values indicate that under dynamic loading, the system reaches its strength capacity earlier, but the ductility is more limited compared to static loading. The energy dissipation mechanisms at the fiber–matrix interface are not fully activated under rapid loading, leading to earlier failure.

The energy absorption capacity values obtained by calculating the areas under the curves presented in Figure 9 were compared for 7- and 28-day specimens under both static and dynamic loading conditions. These values indicate the energy that the material can store before fracture. For the 7-day specimens, the energy absorption capacity was 4.95 kJ/mm³ under static loading and 5.12 kJ/mm³ under dynamic loading, indicating that at early ages the material exhibited slightly higher energy absorption under dynamic conditions similar to studies in the literature [12]. This difference can be attributed to the matrix, which had not yet completed full hydration, retaining its flexibility and the 3D textile reinforcement playing a more effective role in stress transfer. In the 28-day specimens, the energy absorption capacity decreased to 4.32 kJ/mm³ under static loading and to 3.30 kJ/mm³ under dynamic loading. This notable reduction suggests that the material became more brittle with age, and its ductility under high loading rates diminished. After full hydration, the hardening of the cementitious matrix reduced the deformation compatibility between the textile and the matrix, leading to a drop in energy absorption capacity. These findings reveal that the optimum energy absorption capacity in 3D textile-reinforced cementitious composites is achieved at early ages, while at later ages the brittleness of the matrix may lower performance under impact or repeated loading.

A common feature of the stress–strain curves is the presence of a prolonged plastic deformation phase after the elastic region across all specimens. This demonstrates that the 3D textile reinforcement effectively controls crack propagation and maintains load transfer through the fibers. Additionally, higher deformation capacities at early ages and increased stiffness and strength at later ages are observed. Increasing loading rate generally enhances strength but reduces deformation capacity. This combination of ductility and strength suggests that the composite is suitable for a wide range of structural applications requiring both flexibility and strength.

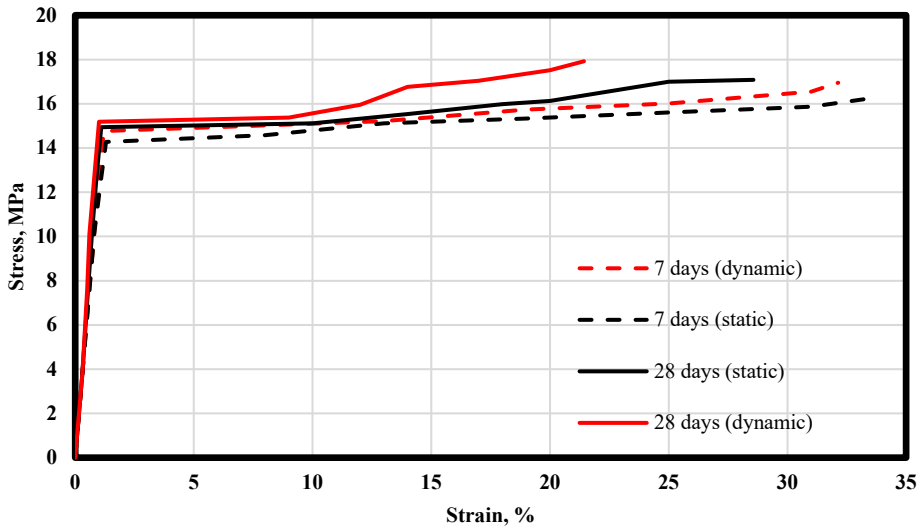

Figure 9. Stress-strain curve of of 3D Textile composite specimens

4. Conclusion

The results obtained from the study are listed below:

- The developed cementitious composite reinforced with 3D textile and waterproof membrane demonstrated a lightweight yet high mechanical performance, highlighting its potential as a durable and lightweight construction material.
- Bending strength increased by over 900% (from 1.68 MPa to 16.95 MPa) between 7 and 28 days, reflecting the effective mechanical interaction between matrix hydration and textile fibers.
- High tensile strength and elongation values under both dynamic and static loading conditions indicate that the material exhibits ductile and energy-absorbing behavior across different strain rates.
- Stress–strain analyses revealed that the composite provides high deformation capacity at early ages along with increased stiffness and strength at later ages, while loading rate significantly influences both strength and ductility.
- The 3D textile effectively controls crack propagation, and the moisture-retaining waterproof membrane supports the composite's long-term mechanical performance, making it suitable for practical applications.

Experimental results demonstrated that the material exhibits ductile, durable, and high energy absorption behavior under various loading conditions. In particular, the effective crack control provided by the textile reinforcement and the moisture-retaining effect of the membrane enhance the long-term performance of the composite, broadening its potential applications. Future studies should focus on detailed investigations of the composite's performance under different environmental conditions, aging effects, and scale-up applications to further expand its structural and functional usage potential.

Declaration of Conflict of Interests

The authors declare that there is no conflict of interest. They have no known competing financial interests or personal relationships that could have appeared to influence the work reported in this paper.

References

[1.] Al-Lami, K., D'Antino, T., Colombi, P., Durability of textile-reinforced cementitious matrix (FRCM) composites: A review. Applied Sciences 10(5) (2020)1714. https://doi.org/10.3390/app10051714

[2.] Hassan, H. Z., Saeed, N. M., Advancements and applications of lightweight structures: a comprehensive review. Discover Civil Engineering, 1(1) (2024)47. https://doi.org/10.1007/s44290-024-00049-z

[3.] Wu, C., Pan, Y., Yan, L., Mechanical properties and durability of textile reinforced concrete (TRC)—a review. Polymers, 15(18) (2023)3826. https://doi.org/10.3390/polym15183826

[4.] Halvaei, M., Fibers and textiles reinforced cementitious composites. In Engineered polymeric fibrous materials (pp. 73-92) (2021) Woodhead Publishing. https://doi.org/10.1016/B978-0-12-824381-7.00001-9

[5.] Pham, H. H., Dinh, N. H., Kim, S. H., Park, S. H., Choi, K. K., Tensile behavioral characteristics of lightweight carbon textile-reinforced cementitious composites. Journal of Building Engineering, 57 (2022) 104848. https://doi.org/10.1016/j.jobe.2022.104848

[6.] Hasan, K. F., Horváth, P. G., Alpár, T., Potential textile-reinforced composites: a comprehensive review. Journal of Materials Science, 56(26) (2021) 14381-14415. https://doi.org/10.1007/s10853-021-06177-6

[7.] Zhang, X., Wang, X., Liang, X., Zhang, Y., Wu, Z., Effect of impregnated polymer type on the mechanical performance of basalt fiber textiles and cement-based composites. Archives of Civil and Mechanical Engineering, 25(3) (2025) 138. https://doi.org/10.1007/s43452-025-01193-8

[8.] Mouritz, A. P., Bannister, M. K., Falzon, P. J., Leong, K. H., Review of applications for advanced three-dimensional fibre textile composites. Composites Part A: applied science and manufacturing, 30(12) (1999) 1445-1461. https://doi.org/10.1016/S1359-835X(99)00034-2

[9.] Misnon, M. I., Islam, M. M., Epaarachchi, J. A., Lau, K. T., Potentiality of utilising natural textile materials for engineering composites applications. Materials & Design, 59 (2014) 359-368. https://doi.org/10.1016/j.matdes.2014.03.022

[10.] Han, F., Chen, H., Li, X., Bao, B., Lv, T., Zhang, W., Hui, D. W., Improvement of mechanical properties of concrete canvas by anhydrite-modified calcium sulfoaluminate cement. Journal of Composite Materials 50(14) (2016a) 1937-1950. https://doi.org/10.1177/0021998315597743

[11.] Han, F., Chen, H., Zhang, W., Lv, T., Yang, Y., Influence of 3D spacer textile on drying shrinkage of concrete canvas. Journal of Industrial Textiles 45(6) (2016b) 1457-1476. https://doi.org/10.1177/1528083714562087

[12.] Xiang, Z., Wang, J., Niu, J., Zhou, J., & Wang, J., Experimental study on the mechanical properties of concrete canvas and CFRP jointly confined circular concrete columns under axial compression. Construction and Building Materials, 385 (2023) 130800. https://doi.org/10.1016/j.conbuildmat.2023.130800

How to Cite This Article

Aybar, K., Ünal, S., Karagöz, Ö., and Canbaz, M., Development of a Flexible, Shape-Adaptive and Waterproof Cementitious Composite Reinforced with 3D Textile. Brilliant Engineering 3(2025), 41049.
https://doi.org/10.36937/ben.2025.41049